DESIGN OF MULTI-CHANNEL CORROSION DETECTION SYSTEM FOR GROUNDING GRID IN SUBSTATION

Yingtian ZHANG[1], Bowen GUO[2], Xin HE[3], Chi ZHANG[4], Songyuan LI[5], Pengfei LI[6,*]

To improve the efficiency and accuracy of corrosion detection of substation grounding grid, a multi-channel corrosion detection system was developed. Based on the Tellegen's theorem, the corrosion diagnosis model was established. The diagnosis model was solved to locate the corrosion branch of the grounding grid accurately by Monte Carlo algorithm and Particle Swarm Optimization algorithm. A grounding grid corrosion detection system with 16 measurement channels was developed using a switch matrix structure, which could measure 120 port resistances simultaneously. The model of the grounding grid was established using Visio. The host computer software was developed based on C#, to achieve the functions of human-computer interaction, computing and others. A field test was carried out in a 110kV substation in Tianjin city, two severely corroded branches were located effectively. The results show that the grounding grid corrosion detection system can locate the corrosion of the grounding grid accurately.

Keywords: Substation grounding grid; corrosion state; multi-channel; detection system

1. Introduction

The grounding grid of substation represents an important measure to ensure the safe and reliable operation of the power system. The grounding grid provides the discharge channel for fault current and lightning current and provides a zero potential reference to ensure stable operation of electrical equipment and

[1] Tianjin Power Technology Development Co., Ltd, Tianjin 300000, China. E-mail: 505129842@qq.com
[2] Tianjin Power Supply Company of State Grid Corporation of China, Tianjin 300000, China. E-mail: 646365392@qq.com
[3] Tianjin Power Technology Development Co., Ltd, Tianjin 300000, China. E-mail: XINH2008@163.com
[4] Tianjin Power Supply Company of State Grid Corporation of China, Tianjin 300000, China. E-mail: zhangchi_tj@126.com
[5] Tianjin Power Technology Development Co., Ltd, Tianjin 300000, China. E-mail: lisongyuan1987@163.com
[6] School of Electrical and Mechanical Engineering, Pingdingshan University, Pingdingshan 467000, China. E-mail: pengfei9966@126.com
*Corresponding Author: Pengfei LI

personnel safety [1-2]. The grounding grid is generally welded by flat steel or flat copper. Corrosion occurs in the grounding grid branch due to long-term soil environmental corrosion and current discharge. In special cases, the grounding grid branch is corroded and fractured, seriously affecting performance of the grounding grid. Therefore, detection of grounding grid corrosion carries important engineering significance [3].

There are mainly the following grounding grid corrosion diagnosis techniques: electric network analysis method [4], electromagnetic field analysis method [5] and soil physical and chemical property analysis method [6]. DL/T1532-2016 (Technical guide for corrosion diagnosis of grounding grid) has proposed relevant technical guidelines for the corrosion degree of grounding grid [7]. It is recommended in the guidelines to use the DC resistance between any two accessible nodes and combine the grounding grid topology to diagnose the corrosion degree. The guidelines also recommend the use of earth continuity tester for port resistance measurement. GB/T28030-2011 (Earth continuity tester) has made relevant provisions on the accuracy, electromagnetic compatibility, measurement and calibration methods for the earth continuity tester [8]. The earth continuity tester principle is to apply a constant current to the grounding grid port, measure the port voltage, and then calculate the port resistance [9]. The overall architecture mainly consists of power module, current output module, signal conditioning acquisition module, MCU module, display and output module [9]. Structurally, the commercial earth continuity tester includes a current output channel and a voltage acquisition channel, which measures the resistance of one port at a time. Previous studies have shown that excessive port resistances need to be measured for corrosion detection of substation grounding grids [10]. Using the current commercial earth continuity tester for total station measurement faces problems such as huge engineering volume, cumbersome data recording and low measurement efficiency.

In this paper, a multi-channel grounding grid corrosion detection system is developed. On the basis of Tellegen's Theorem, the grounding grid corrosion diagnosis model is built. The Monte Carlo (MC) -Particle Swarm Optimization (PSO) algorithm is proposed to solve the diagnosis model. First, the solution space is constrained using MC algorithm, and an accurater results are obtained by the PSO algorithm. The architecture of the multi-channel grounding grid corrosion detection system is proposed. The continuous multi-channel measurement is possible by building channel switching matrix using relays and analog switches with pilot frequency AC constant current power source as the current source. The grounding grid model is built by Visio, and human-computer interaction and fault diagnosis are possible based on upper computer software developed with C#. A multi-channel grounding grid corrosion detection system is developed and field-tested in a 110kV substation to verify accuracy of the system.

2. Principle of corrosion detection for substation grounding grid

2.1 The diagnosis model of the grounding grid

The substation grounding grid can be simplified into the equivalent resistance network shown in Fig.1(a). The grounding grid corrosion leads to an increase in the corresponding branch resistance. The nature of the corrosion diagnosis is to measure the resistance changes in each branch of the grounding grid [11]. The topology of the grounding grid has not changed before and after corrosion. It is assumed that the circuits of the topological structure before and after the corrosion are N and N' (as shown in Fig.1(b)), the corresponding branches and nodes take the same number, and the reference directions of the corresponding branches are the same, then according to the Tellegen's theorem [12], there is:

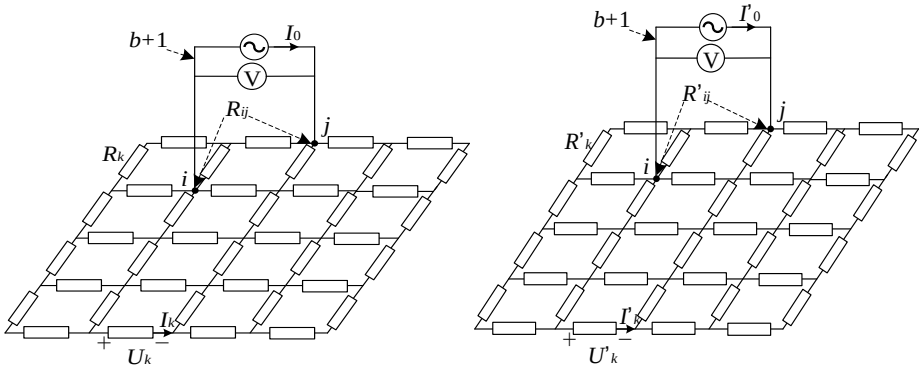

(a) topological structure N (b) topological structure N'

Fig.1 Grounding grid topology.

$$\begin{cases} \sum_{k=1}^{b} U_k' I_k = 0 \\ \sum_{k=1}^{b} U_k I_k' = 0 \end{cases} \tag{1}$$

In the formula, k is the breach No., b is the total number of the grounding grid. I_k and U_k are the branch current and branch voltage of the electric network N, respectively, I'_k, U'_k are the branch current and branch voltage of the electric network N', respectively. For any resistor network, if the network topology and branch resistance are known, the port resistance can be obtained according to the node analysis method. For the corroded network, the port resistance can be obtained by measurement, and the branch resistance is then obtained by backward reasoning of the port resistance.

The grounding grid before corrosion can be regarded as a network N having b+1 branches and n nodes. Wherein, the b+1th branch is a constant current source

branch connected to the i, j nodes of the earthing network, and the current value is I_0.

By measuring the voltage between the i and j nodes, the port resistance value R_{ij} is obtained after calculation. By applying the same constant current source I_0 to the corresponding i, j nodes in the etched network N', the etched port resistance R'ij can be obtained. Since the topology of the two networks is consistent (even if a branch is corroded and fractured, the branch resistance can be regarded as infinite), the difference between the two networks lies in different branch resistance values. According to the Tellegen's theorem [14], there is:

$$\begin{cases} \sum_{k=1}^{b+1} U_k I_k^{'} = 0 \\ \sum_{k=1}^{b+1} U_k^{'} I_k = 0 \end{cases} \tag{2}$$

The current of the b+1th branch of i, j nodes is I_0 for both networks, and it is substituted into equation (2) to obtain:

$$\begin{cases} R_{ij} I_0^2 = \sum_{k=1}^{b} U_k^{'} I_k \\ R_{ij}^{'} I_0^2 = \sum_{k=1}^{b} U_k I_k^{'} \end{cases} \tag{3}$$

It is defined that the port resistance increment is $\Delta R_{ij}=R'_{ij}-R_{ij}$ and the branch resistance increment is $\Delta R_k=R'_k-R_k$. The two equations in the formula (3) are subtracted to obtain the Eq.(4).

$$\Delta R_{ij} = \sum_{k=1}^{b} \Delta R_k I_k I_k^{'} \Big/ I_0^2 \tag{4}$$

Equation (4) shows the relationship between the branch resistance variation and the port resistance variation. Assume that the network has m accessible nodes, then up to $\varepsilon(\varepsilon=C_m^2)$ port resistance values can be obtained, so it is possible to construct an ε-dimensional fault diagnosis equation set as shown in Eq.(5).

$$\begin{cases} \Delta R_{ij(1)} = \sum_{k=1}^{b} \Delta R_k I_{k(1)} I_{k(1)}^{'} \big/ I_0^2 \\ \Delta R_{ij(2)} = \sum_{k=1}^{b} \Delta R_k I_{k(2)} I_{k(2)}^{'} \big/ I_0^2 \\ \qquad\qquad \vdots \\ \Delta R_{ij(\varepsilon)} = \sum_{k=1}^{b} \Delta R_k I_{k(\varepsilon)} I_{k(\varepsilon)}^{'} \big/ I_0^2 \end{cases} \tag{5}$$

Where, I_0, I_k in the equation set are known. ΔR_k, R'_k are unknown variables. I'_k is to be determined depending on R'_k. By using a suitable

optimization algorithm to solve the mathematical model, the resistance value of each part of the conductor after the fault can be obtained to judge its corrosion.

2.2 Solution for fault diagnosis equations based on MC-PSO algorithm

To obtain an accurate diagnosis results, a constraint optimization target is constructed, as shown in Eq. (6). Where, the $\Delta \hat{R}_{ij(\varepsilon)}$ is the port resistance of the grid N' with the branch resistance $\Delta \hat{R}_1, \Delta \hat{R}_2, \cdots, \Delta \hat{R}_b$, which is the solution of Eq.(5). The optimization target is to find a set of solutions of Eq.(5) to minimize the Euclidean distance between $\Delta \hat{R}_{ij(\varepsilon)}$ and $\Delta R_{ij(\varepsilon)}$.

$$\min f\left(\Delta \hat{R}_1, \Delta \hat{R}_2, \cdots, \Delta \hat{R}_b\right) = \sum_{k=1}^{\varepsilon}\left(\Delta \hat{R}_{ij(\varepsilon)} - \Delta R_{ij(\varepsilon)}\right)^2 \tag{6}$$

In engineering, there are three unknown issues when corrosion occurs: first, the number of corrosion branches is unknown; second, the location of corrosion branch is unknown; and third, the corrosion degree of the corrosion branch is unknown. It is easy to fall into a local optimal solution when directly solving Eq. (5) by optimization algorithm with the optimization target. Because the number, location, and amplitude of the changed individuals are random in each iteration, and the Eq. (6) cannot provide effective iteration direction. Meanwhile, Eq. (5) is an underdetermined equations with infinite groups of solutions. For traditional algorithms, the initial value is randomly, and the results will fall into a locally optimal solution, so effective results are impossible.

The MC-PSO algorithm is used to improve the accuracy [13-15]. Firstly, the number and location of the corrosion branches are locked in a fixed range through the MC algorithm. Secondly, the PSO algorithm is used to optimize the variation of branch resistance to obtain an accurate degree of corrosion. Specific steps are as follows:

Step 1: Searching the number of corrosion branches based on MC algorithm.

S1.1: Randomly initialize multiple groups of $\Delta \mathbf{R}_k$. Only initialize the number of each group $\mathbf{\Delta R_k}$. The initialization method is as follows: all elements in each group $\mathbf{\Delta R_k}$ are randomly sorted, and value of the first d elements is assigned ($d \leq b$). According to the corrosion discrimination standard specified by DL/T1532-2016, the assignment is one of the multiples at 2~50 times of the theoretical resistance of each branch;

S1.2: The port resistance $\Delta \hat{R}_{ij}$ of the grid N' is calculated by the initialized $\mathbf{\Delta R_k}$ according to the electrical network theory [16], then the fitness of each group $\mathbf{\Delta R_k}$ are calculated the by Eq.(6);

S1.3: Count the number of assignment branches D corresponding to the minimum fitness;

S1.4: Steps S1.1-S1.3 are repeated p times and calculating the fitness. The value of D_p corresponding to the minimum fitness is the number of corrosion branches.

Step 2: Searching the branch No. of the corrosion branches based on MC algorithm.

S2.1: Randomly initialize multiple groups of ΔR_k. Only initialize the positions of each group $\mathbf{\Delta R_k}$. The initialization method is as follows: *b* elements in each $\mathbf{\Delta R_k}$ are randomly sorted, and the first D elements are sequentially assigned. The assignment method is same as S1.1. The assigned branch No. are recorded;

S2.2: The port resistance ΔR_{ij} of the grid N' is calculated by the initialized $\mathbf{\Delta R_k}$, then calculating the fitness by Eq. (6);

S2.3: Record the assignment branch No. which correspond to the minimum fitness;

S2.4: Steps S2.1-S2.3 are repeated q times. The frequency of the branch No. is counted, The C_q branches with the highest frequency are extracted, which are the corrosion branches. C_q is equal to D_p normally.

Step 3: Calculating the corrosion degree of the corrosion branches by PSO algorithm

S3.1: Particle initialization. Set the population dimension to *b*, the population number to *Q*, and the maximum number of iterations to W. Generate initialization particles $\mathbf{\Delta R_k}=(\Delta R_1, \Delta R_2,...,\Delta R_b)$, and assign a random number within 2~50 times of the theoretical resistance value to the particles which correspond to the corrosion branches No., and that smaller than 2 times of the theoretical resistance value is assigned to the others particles;

S3.2: Fitness calculation. The branch current $\mathbf{I_k^t}$ is calculated based on the initialized particles by electric network theory [16]. Where, *t* is the number of iterations. Substitute $\mathbf{I_k^t}$ and $\mathbf{\Delta R_k^t}$ into Eq.(5) to calculate $\mathbf{\Delta R_{ij}^t}$; then substitute them into Eq.(6) to calculate the fitness. Record the global optimal fitness g_{best} and optimal fitness p_{best};

S3.3: Updating the value of the particles. Update the particles according to Eq.(7) and Eq.(8). The updated range of the particles corresponding to the corrosion branches is 2~50 times of the theoretical resistance value, and the update range of the remaining particles shall not exceed 2 times of the theoretical resistance value. If it exceeds, keep the original value;

$$v_k^{t+1} = v_k^t + c_1 rand_1\left(p_{best}^t - \Delta R_k^t\right) + c_2 rand_2\left(g_{best}^t - \Delta R_k^t\right) \tag{7}$$

$$\Delta R_k^{t+1} = \Delta R_k^t + v_k^{t+1} \tag{8}$$

S3.4: Recalculate the fitness of the particles updated in step S3.3. When the fitness is less than a certain value or reaches the number of iterations, the optimal

particle is output, which is the solution of equation (5). Otherwise, repeat steps S3.2-S3.3.

With the three steps above, the localization and degree of the corrosion branch can be obtained accurately.

3. Design of the detection system

3.1 Design of the system architecture

It can be known from the above theory that in order to accurately determine the corrosion of the grounding grid, it is necessary to obtain as many port resistances of the grounding grid as possible. To this end, the principle of multi-channel substation grounding grid corrosion detection system is proposed herein as shown in Fig.2.

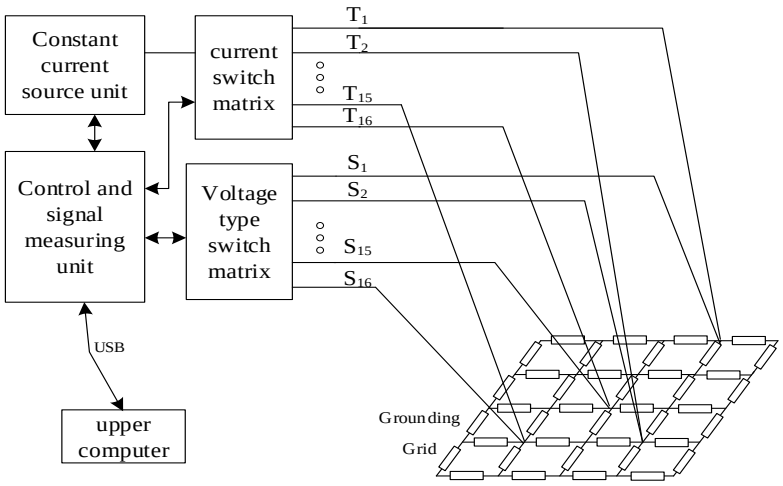

Fig.2 Functional block diagram of the detection system.

It can be seen from Fig.2 that the system designs 16 measurement channels, including the lower computer measurement system and the Upper computer software. The lower computer measurement system includes an AC constant current source unit, a control and signal measuring unit, and a current and voltage signal switch matrix. The lower computer realizes functions such as current output, voltage acquisition, resistance calculation and channel switching. The Upper computer software realizes functions such as human-computer interaction, model input and corrosion calculation. The upper computer and the lower computer communicate via the USB interface. The output of the AC constant current source in Fig.2 is applied to any two down-conductor ports through the current switch matrix, and the voltage signal switch matrix switches the corresponding voltage signal to control and signal detection unit. By

permutation and combination, up to 120 port resistance measurements can be made at one time.

3.2 Design of upper computer control system

The upper computer plays a role in human-computer interaction, lower computer control, grounding grid model construction, measurement data reading and diagnostic equation solving, etc. The upper computer is developed based on C# and the functional flow chart is shown in Fig.8.

The system module functions are described as follows:

(1) Modeling module: Using the secondary development interface of Microsoft Office 2013, Visio 2013 is invoked to draw the basic model of the substation grounding grid.
(2) Measurement module: The lower computer is used to complete the wiring of the countable node in the field, and the upper computer is started to automatically complete the measurement work.
(3) Calculation module: Through the form of dynamic link library, the algorithm module is invoked to complete the data analysis.
(4) Display module: According to the preset threshold, the grounding grid is alerted by different colors in the model diagram.

In order to standardize the operation process and simplify the substation site measurement steps, the upper computer system interface design integrates the above four functional modules into one main program, and the interface is as shown in Fig.3:

According to the above design scheme, the detection system is as shown in Fig.4(a). In Fig.4(b), an earth continuity tester is listed, and the model number is HTDT-10A, which is the recommended measuring instrument of the standard DL / T1532-2016 (Technical guide for corrosion diagnosis of grounding grid) and meets the requires of the GB / T28030-2011 (Earth continuity tester). The earth continuity tester has a measuring channel only. Compared with the earth continuity tester, the designed system in this paper has two advantages. The first is that the measurement efficiency is improved. 120 port resistances can be measured continuously with only one connection, however, to complete the same workload, the earth continuity tester needs to measure 120 times. The second advantage is the corrosion branches of the grounding grid can be located after the measurement directly. The port resistance values are recorded and stored by the Upper computer software while measuring, and the corrosion branches are located by the diagnostic algorithm with the model of the grounding grid and the measuring results. But, the measuring value of the earth continuity tester should be recorded manually, and the corrosion branches cannot be obtained, because the port resistance is influenced by all the branches.

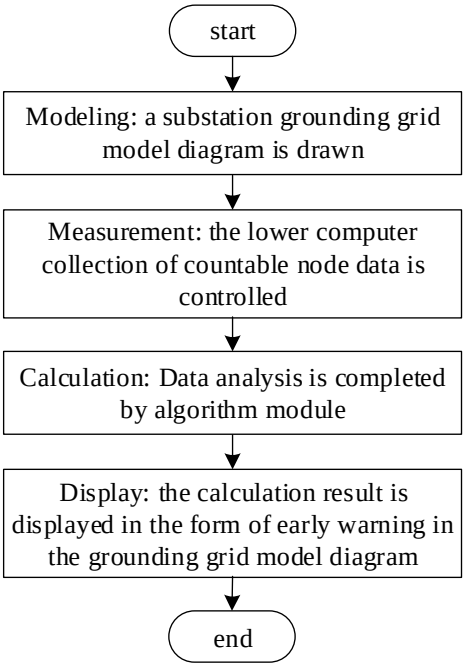

Fig.3 Upper computer function flow chart.

(a) The multi-channel corrosion detection system (b) The earth continuity tester

Fig.4 The designed system and the earth continuity tester.

4. The field test in substation

4.1 Field test

To verify the designed system, a field test was performed in a 110kV substation in Tianjin, China. The substation test site is shown in Fig.5.

Fig.5 The field test site.

The substation built in 2005 covers an area of 17,550 m^2. The grounding grid consists of four areas: 110kV switching field area, main transformer and 10kV switching room area, 35kV switching field area, and capacitor area. The grounding grid is welded using 40*6mm flat steel with buried depth of 0.8m. The grounding grid model is shown in Fig. 6, which was created by Visio.

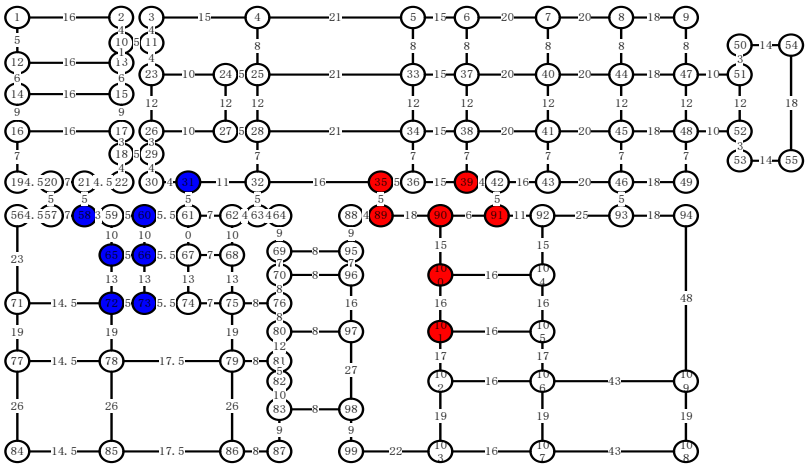

Fig.6 The modeling of the grounding grid.

The circle in the figure represents the grounding grid node, and the number on the connection line between the nodes represents the length of the grounding grid branch, unit: m. The grounding grid has 109 nodes and 161 branches. Due to the large area of the substation, the four field areas were measured separately, and a total of 53 accessible nodes were measured. 16, 12, 14, and 11 accessible nodes were measured in the four areas, and a total of 332 port resistance values were obtained.

4.2 Test results and analysis

Due to the large amount of measurement data, only the data of the ports with detection abnormalities are listed, and all measurement data are taken for calculation. The nodes labeled in blue and those labeled in red in Fig. 6 are partial accessible nodes detected in the second and third areas, respectively. The blue nodes are marked as 31, 58, 60, 65, 66, 72, 73, while the red nodes are marked as 35, 39, 89, 90, 91, 100, 101. The port resistance measured in the two areas and the theoretical resistance are listed in Tab.1.

Table.1

The theoretical and measured values of port resistance (unit: mΩ)

Port No.	Theoretical resistance	Measured resistance	Port No.	Theoretical resistance	Measured resistance
31-58	4.61	6.01	35-39	5.16	6.37
31-60	3.63	4.98	35-89	2.37	3.69
31-65	5.06	142.11	35-90	6.40	7.85
31-66	4.31	5.57	35-91	6.30	7.48
31-72	5.91	7.24	35-100	10.40	16.23
31-73	5.58	6.81	35-101	13.02	16.70
58-60	3.11	4.54	39-89	5.86	7.28
58-65	4.09	141.23	39-90	4.97	6.77
58-66	4.08	5.37	39-91	3.59	4.96
58-72	5.44	6.82	39-100	8.70	14.91
58-73	5.44	6.72	39-101	11.44	15.58
60-65	3.33	140.18	89-90	5.91	7.27
60-66	2.62	3.66	89-91	6.25	7.53
60-72	4.73	5.93	89-100	10.13	15.68
60-73	4.45	5.52	89-101	12.83	16.78
65-66	2.00	138.71	90-91	2.36	3.86
65-72	3.61	140.54	90-100	5.84	13.70
65-73	3.78	140.54	90-101	9.56	14.8
66-72	3.59	4.64	91-100	6.52	12.9
66-73	3.08	4.01	91-101	9.67	13.89
72-73	2.19	3.17	100-101	6.04	7.32

As can be known from Tab.1, in the second area, all the port resistances related to node 65 increase by more than 30 times, while the remaining are not much increased. In the third area, resistance of each port is increased, but the

increase is not large. A diagnosis model is established based on the algorithm proposed in Section 2.1. Firstly, search the number of corrosion branches according to MC algorithm as step 1 in Section 2.2. Set the particle dimension to 161. According to the preliminary analysis of the detection results, set d=6, and set the number of assignment $\mathbf{\Delta R_k}$ to 500, 100, 5000, 10000, 20000, 30000, and 40000, and set the execution times p=10. The fitness of the results is shown in Tab. 2. When D=4, 7 values of the fitness reach the minimal, and it can be known that there are 4 branches where corrosion occurs. Secondly, search for the branch No. according to step 2.

Randomly assign the first 4 random-ordered branches 500 groups and set q=1000. Partial statistical results of the assignment branch No. are shown in Tab. 3. It can be known that the corrosion branches may be 59-65, 65-66, 65-72, 90-100. Optimize the degree of corrosion according to step 3. Set the number of particles to 500, set the maximum number of iterations to 1000, and optimize resistance of the four branches of 59-65, 65-66, 65-72, and 90-100. Partial optimization results are shown in Tab. 4. The branches' resistance of 59-65, 65-66, and 65-72 increases by more than 26 times, while that of 90-100 branches increases by more than 4 times.

Node 65 is the grounding wire of the 110kV arrester, and branch 90-100 is the grounding grid between the earth point of #1 main transformer core and the 35kV isolation switcher. These two branches are excavated, with results shown in Fig.7(a) and (b).

Table 2

The statistics of the number of corrosion branch

Cycle No.	D=1	D=2	D=3	D=4	D=5	D=6
1	1.371	0.922	1.047	0.669	0.861	1.371
2	0.861	0.861	1.052	1.058	1.148	0.861
3	1.148	1.148	0.957	0.924	0.931	1.148
4	0.931	1.123	1.009	0.957	1.111	0.931
5	0.957	0.754	0.896	0.957	1.135	0.957
6	1.135	1.135	0.845	1.082	1.133	1.135
7	1.133	1.171	1.146	0.595	0.956	1.133
8	1.087	0.754	0.998	0.547	1.146	1.087
9	1.146	1.146	0.936	1.060	1.030	1.146
10	1.099	0.814	0.933	0.734	1.011	1.099

Table 3

The statistics of the branch No. Of the corrosion branch

Branch No.	59-65	65-66	65-72	90-100	91-90
Frequency	627	387	342	296	92

Table 4

The resistance of the corrosion branch

Branch No.	59-65	65-66	65-72	100-101

Theoretical resistance[mΩ}	5.75	2.875	7.475	8.625
Calculation result[mΩ]	168.36	130.01	207.78	43.47
Increase times	28.28	44.22	26.80	4.04

(a) Excavation result of No. 65 down conductor (b) Excavation result of nodes 90-100

Fig.7 Grounding grid excavation result.

There are two severe corrosion points on the grounding wire of the node 65, both of which are almost fractured, and the second corrosion point was broken during the excavation. The grounding flat steel between 90-100 nodes is subject to nearly 60% corrosion. Since the grounding wire is connected to the grounding grid, the grounding grid below node 65 has no corrosion. This is the reason that the port resistance related to node 65 is significantly increased, while the port resistance irrelevant with node 65 is not increased much.

5. Conclusion

In this paper, a diagnosis algorithm for multi-channel substation grounding grid corrosion detection system is proposed, and the software and hardware systems are developed. The system has been applied in a 110kV substation. The conclusions are summarized as follows:

(1) The grounding grid corrosion diagnosis model was established based on Tellegen's Theorem, and the solution to underdetermined equations of the diagnosis model is proposed based on MC-PSO algorithm. The problems of improper setting of initial value and easy fall into locally optimal solution are solved, and the accuracy of the solution is improved;

(2) Multi-channel grounding grid corrosion detection system is designed. Simultaneous measurement of multiple ports is achieved using voltage and current switch matrixes. Grounding grid modeling based on Visio achieves effective conversion of grounding grid and the calculation model, greatly improving the field detection efficiency;

(3) A field test was carried in a 110 kV substation, and two severe corrosion branches were found effectively. The results show that the multi-channel substation grounding grid corrosion detection system can accurately locate the position where the grounding grid has corrosion.

REFERENCES

[1]. *Colominas I, Navarrina F, Casteleiro M*. Numerical simulation of transferred potentials in earthing grids considering layered soil models, J.IEEE Transactions on Power Delivery, **vol.** 22, no. 3, Feb. 2007, pp. 1514-1522.

[2]. *Qamar A, Shah N, Kaleem Z.* Breakpoint diagnosis of substation grounding grid using derivative method, J. Progress In Electromagnetics Research, **vol.** 57, May. 2017, pp. 73-80.

[3]. *M. Mitolo, A. Pettinger*. Interactions between cathodically protected pipelines and grounding systems. 2016 IEEE/IAS 52nd Industrial and Commercial Power Systems Technical Conference (I&CPS), Detroit, 2016, pp. 1-6.

[4]. *Xu Lei, Li Lin*. Corrosion and breakpoint diagnosis method for substation grounding grid based on electric network theory, J. Transactions of China Electrotechnical Society, **Vol**. 27 No. 10, Oct. 2012, pp. 270-276.

[5]. *C R Ratto, P A Torrione, L M Collins*. Exploiting ground-penetrating radar phenomenology in a context-dependent framework for landmine detection and discrimination, J. IEEE Transactions on Geoscience & Remote Sensing, **Vol**. 49 No. 5, May. 2011, pp. 1689-1700.

[6]. *Li Xingde, Li Xiaojuan, Yang Jie, et al*. The Grounding Grid Corrosion Comparative Judgment and Difference Analysis Using Different Soil Corrosion Evaluation Methods, J. Electric Power Technology and Environmental Protection, **Vol**. 30 No. 6, Dec. 2014, pp. 8-9.

[7]. DL/T1532-2016 Technical guidelines for grounding grid corrosion diagnosis

[8]. GBT28030-2011 Earth continuity tester.

[9]. *Tang Huiqiang, Ge Lili, Jing Hua*. Ground Resistance Detection System Based on Wireless Sensor Network. J. Instrument Technique and Sensor, **Vol**. 15 No. 2, Feb. 2015, pp. 54-56.

[10]. *Liu Yugen, Tian Zi, Lei Chao, et al*. Conductor Loss Diagnosis of Grounding Grid Based on Binary Genetic Algorithm, J. High Voltage Engineering, **Vol**. 40 No. 5, May. 2014, pp. 1439-1445.

[11]. *Xu Lei*. Fault Diagnosis for Grounding Grids Based on Electric Network Theory, J. Transactions of China Electrotechnical Society, **Vol**. 27 No. 10, Oct. 2012, pp. 270-276.

[12]. *D. Hazarika*. A Fast Continuation Load Flow Analysis for an Interconnected Power System, J. International Journal of Energy Engineering, **Vol**. 2 No. 4, Nov. 2012, pp. 126-136.

[13]. *Gatta F M, Geri A, Lauria S.* Simplified HV tower grounding system model for backflashover simulation, J. Electric power systems research, **Vol**. 85, Apr. 2012, pp. 16-23.

[14]. *Sedghi M, Aliakbar-Golkar M, Haghifam M R.* Distribution network expansion considering distributed generation and storage units using modified PSO algorithm, J. International Journal of Electrical Power & Energy Systems, **Vol**. 52, Nov. 2013, pp. 221-230.

[15]. *Geethanjali M, Slochanal S M R, Bhavani R*. PSO trained ANN-based differential protection scheme for power transformers, J. Neurocomputing, **Vol**. 71, No. 4-6, Jan. 2008, pp. 904-918.

[16]. *Mesbahi M, Egerstedt M*. Graph theoretic methods in multiagent networks [M]. Princeton University Press, 2010.